Investigation on Fault Detection for Split Torque Gearbox Using Acoustic Emission and Vibration Signals

Ruoyu Li [1], David He [1], and Eric Bechhoefer [2]

[1] *Department of Mechanical & Industrial Engineering*
The University of Illinois at Chicago, Chicago, IL, 60607, USA
rli8@uic.edu
davidhe@uic.edu

[2] *Goodrich Sensors & Integrated Systems,Vergennes, VT, 05419, USA*
Eric.Bechhoefer@Goodrich.com

ABSTRACT

When compared with a traditional planetary gearbox, the split torque gearbox (STG) potentially offers lower weight, increased reliability, and improved efficiency. These benefits have driven the helicopter manufacturing community to develop products using the STG. However, this may pose a challenge for the current gear analysis methods used in Health and Usage Monitoring Systems (HUMS). Gear analysis uses time synchronous averages to separates in frequency gears that are physically close to a sensor. The effect of a large number of synchronous components (gears or bearing) in close proximity may significantly reduce the fault signal (decreased signal to noise) and therefore reduce the effectiveness of current gear analysis algorithms. As of today, only a limited research on STG fault diagnosis has been conducted.

In this paper, we investigated fault diagnosis for STG using both vibration and acoustic emission (AE) signals. In particular, seeded fault tests on a STG type gearbox were conducted to collect both vibration and AE signals. Gear fault features were extracted from vibration signals using a Hilbert-Huang Transform (HHT) based algorithm and from AE signals using AE analysis, respectively. These fault features were used for fault detection using a K-nearest neighbor (KNN) algorithm. Our investigation has shown that that both vibration and AE signals were capable of detecting the gear fault in a STG. However, in terms of locating the source of the fault, AE analysis outperformed vibration analysis.[*]

1 INTRODUCTION

The requirement for higher energy density transmissions (lower weight) in helicopters has lead to the development of the split torque gearbox (STG) to replace the traditionally planetary gearbox by the drive drain designer (White[1], 1982). In comparison with traditionally planetary gearbox, STG potentially offers the following benefits (White[2], 1982): (1) high ratio of speed reduction at final stage; (2) reduced number of speed reduction stages; (3) lower energy losses; (4) increased reliability of the separate drive paths; (5) fewer gears and bearings; (6) lower noise. These benefits have driven the helicopter manufacturing community to develop products using the STG. For example, the Comanche helicopter was designed with a STG, and the new Sikorsky CH-53K will incorporate the STG design to transmit over 18,000 hps to the rotor blades. It is likely that STG will be incorporated into more designs in the future (Gmirya, 2008).

A simplified split torque gear drawing (White[2], 1982) is shown in Figure 1 and a more representative gearbox design, such that seen in (Krantz, 1996) from the Comanche STG is given in Figure 2.
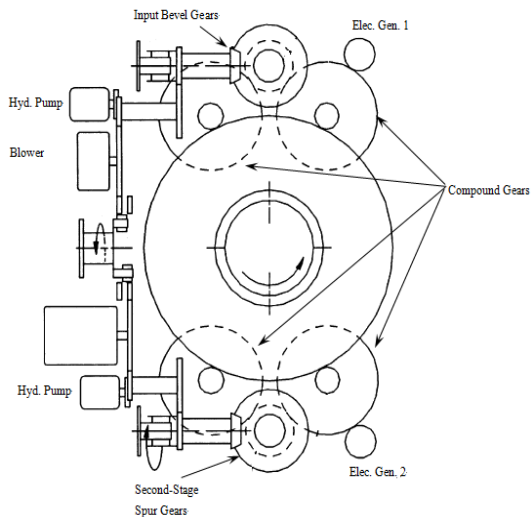

Figure 1: A simplified STG

Figure 2: Comanche STG

Because of the limited experience in building helicopter with STG, there is no condition based monitoring data on this type of gearbox. Studies have been conducted to model and analyze vibration dynamics of the STG (Krantz, 1995), and analysis on gear loading has been conducted (Krantz, 1996). Yet, these studies do not give insight into fault detection of gears on this type of design. Gear diagnostics use time synchronous averages to separates in frequency gears that are physically close. As shown in Figure 1, in a STG, to divide the torque evenly, several identical compound gears will mesh simultaneously with the bull gear. The effect of a large number of synchronous components (gears or bearing) in close proximity may significantly reduce the fault signal (decrease signal to noise ratio) and therefore reduce the effectiveness of current gear analysis algorithms. Only limited research on STG fault diagnosis has been conducted to date. In

a recent paper (Bechhoefer *et al.*, 2009), an investigation on condition indicator performance on a STG type gearbox was reported. In this paper, a number of vibration analysis based condition indicators were tested on detecting seeded gear faults in the gearbox. These condition indicators were generated using a number of vibration analysis techniques including: traditional gear analysis algorithms: time synchronous average (based on both shaft and mesh tones), narrow band signal analysis, Hilbert-Huang transform (HHT), and beam forming. The results of the investigation showed that these condition indicators were effective in detecting a chipped gear tooth in the gearbox. Among those tested, it was shown those condition indicators generated by HHT are powerful in detecting gear fault. No investigation results on how to locate the gear faults were reported in the paper.

In this paper, an investigation on detecting and locating gear faults in a STG using both vibration analysis and acoustic emission analysis is presented. In our investigation, gear fault features will be extracted from vibration signals using a HHT based algorithm. The gear fault features will also be extracted from acoustic emission (AE) signals using traditional AE analysis method. These fault features will be used for fault detection using a K-nearest neighbor (KNN) algorithm. The effectiveness of these methods will be compared using a STG type gearbox seeded fault test data. The remainder of the paper is organized as follows. In Section 2, our investigation approach in general, HHT, AE analysis and KNN are introduced. Section 3 provides a detail description of the experimental setup and analytical results for both vibration and AE signals. Finally, Section 4 concludes the paper.

2 SPLIT TORQUE GEARBOX FAULT DETECTION

In this paper, the fault detection problem for STG using both vibration and AE signals is investigated.

Until now, vibration-based techniques are the most widely used ones for gear fault diagnosis since vibration signals are easy to obtain. In the area of vibration based gear fault detection, it has been proven the time-frequency methods are the most powerful tools. The time-frequency methods include short-time Fourier transform (SFT), Wigner-Ville distribution, wavelet analysis, and HHT. Among these methods, HHT has shown to be effective in fault detection in STG (Bechhoefer *et al.*, 2009). In this paper, the gear fault features will be extracted by an HHT based algorithm.

AE signals are widely used in non-destructive testing (NDT) of static structures, such as bridge, metal structures. Recently, it has been extended to health

monitoring of rotating machines (Tan *et al.*, 2007). Comparing with the vibration signals, AE signals have the following advantages: (1) Insensitive to structural resonances and unaffected by typical mechanical background noise, (2) More sensitive to activity from faults, (3) Provides good trending parameters, (4) Localization of measurements to the machine being monitored. These advantages make the acoustic emission based fault diagnostics technique potentially more competitive than the vibration based fault diagnostics technique for the split torque transmission train. In this paper, traditional AE analysis is used to extract features from AE signals.
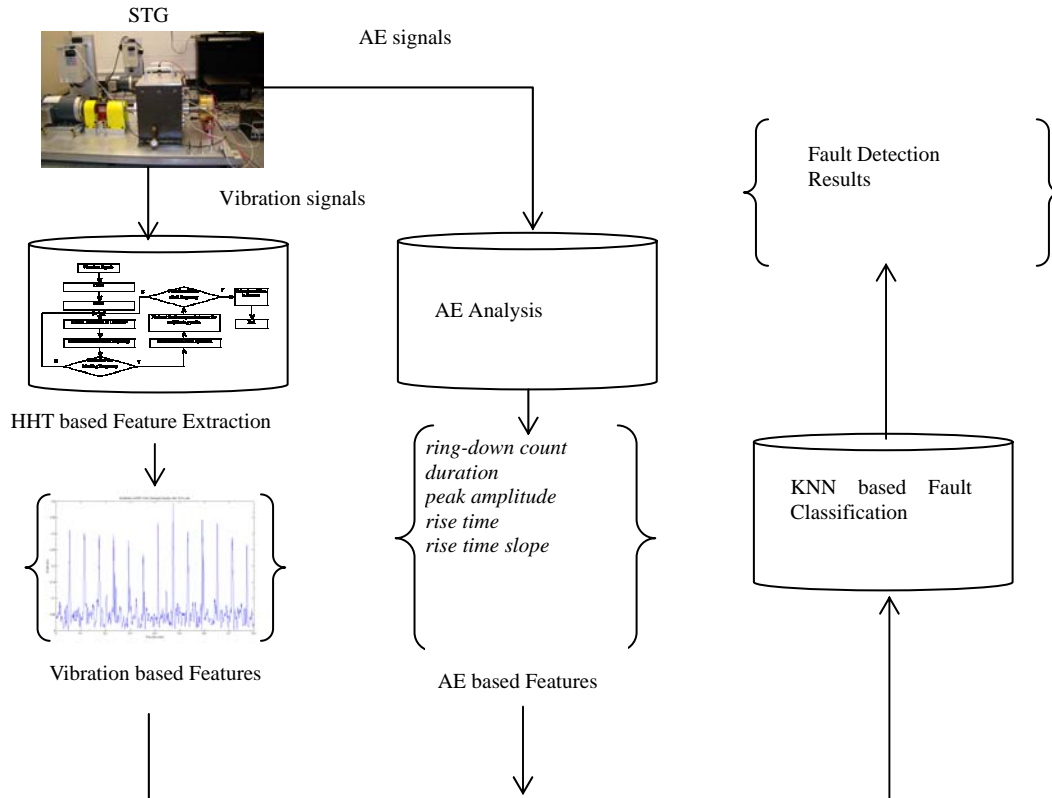

Figure 3: The investigation for STG fault detection

2.1 HHT based Fault Feature Extraction

HHT is first proposed by Huang et al. (Huang *et al.*, 1998). HHT can effectively analyze the non-stationary signals without the uncertainty introduced by selecting a basic function. It has been proven to be effective in various applications, such as rotational machine health diagnosis (Yan and Gao, 2006), (Liu *et al.*, 2006), (Li and He, 2009), structure health monitoring (Liu *et al.*, 2006), bio-tech signals processing (Tang *et al.*, 2007), and so on.

HHT uses empirical mode decomposition (EMD) method to decompose signal into several intrinsic mode functions (IMF). According to Huang et al (Huang *et al.*, 1998), a function $f(t)$ is defined to be an IMF, if it satisfies two characteristic properties: (1) $f(t)$ has exactly one zero between any two consecutive local extrema. (2) $f(t)$ has zero "local mean".

The steps of EMD are provided as below:

1. Find the local maxima and local minima of the signals.

2. Construct the lower and upper envelopes of the signals by the cubic spline respectively based on the local maxima and local minima.

3. Calculate the mean values $m(t)$ by averaging the lower envelope and the upper envelope.

4. Subtract the mean values from the original signals to produce $h_1(t)=f(t)-m(t)$. If it is the true

intrinsic mode function, go to the next step. And the IMF component $C_i(t)=h_m(t)$ is saved. If it is not the IMF, go throughout step 1 to step 4. The stop condition for the iteration proposed in (Huang *et al.*, 1998) is given by Eq. (1).

$$\sum_{t=0}^{T} \frac{[h_{m-1}(t) - h_m(t)]^2}{h^2{}_{m-1}(t)} \le SD \qquad (1)$$

Where $h_{m-1}(t)$ and $h_m(t)$ denote the IMF candidates of the m-1 and m iterations, respectively and Usually *SD* is set between 0.2 and 0.3.

5. Calculate the residual component by subtracting IMF component obtained in step 4 from the original signals $res_i(t)=f(t)-C_i(t)$. This residual component is treated as new data and is subjected to the same processes described above to calculate the next IMF component.

6. Repeat the steps 1-5 until the final residual component becomes a monotonic function and no more IMF component can be extracted or the envelopes becomes smaller than a pre-determined value.

Through step (1) to (6), the original signals *f(t)* can be decomposed into *N* empirical modes (C_1-C_N)and a residue res_N as:

$$f(t) = \sum_{n=1}^{N} C_n + res_N \qquad (2)$$

Once the original signals are decomposed into IMF components, one may analyze the properties of each component by using the Hilbert transform. Since we use HHT to extract fault features in this paper, the scheme of HHT based fault feature extraction (Li and He, 2009) is repeated in Figure 4. As shown in Figure 4, the vibration signals are first decomposed by EMD and then the IMF, which contains the fault information, is selected. The fault features are finally calculated.
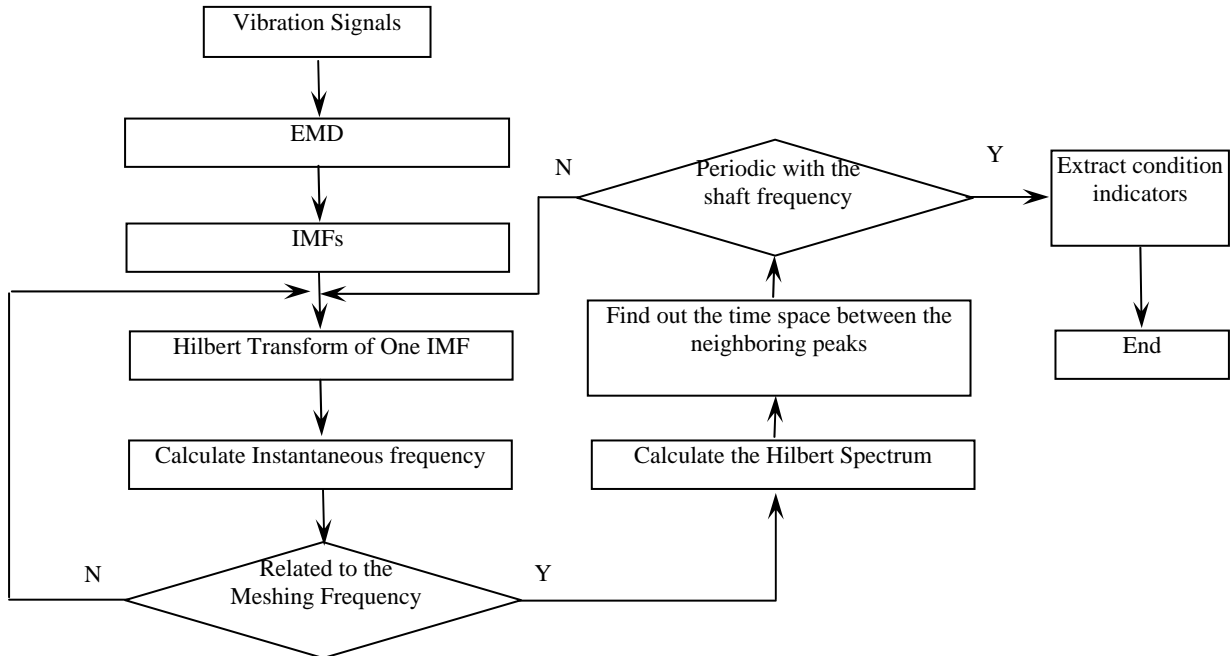

Figure 4: The scheme of the HHT based feature extraction

2.2 AE Analysis based Fault Feature Extraction

Until now, there are three types of approaches for detecting the gear faults: AE analysis, debris monitoring and vibration analysis (Wang *et al.*, 2001). Among them, AE has been shown to be the most sensitive to the gear damage (Eftekhamejad and Mba, 2009), (Toutountzakis *et al.*, 2005), (Hamzah and Mba, 2009).

AE signals from rotating machines usually involve non-stationary, transient characteristics and mixtures of various dynamic events. One challenge in processing AE signals is how to extract the relevant features from a vast dataset, especially if the emitted signals are becomes smaller than a pre-determined value. Fortunately, a typical AE waveform usually illustrates some of the characteristics of an AE signal and therefore correlates to the states of the components being monitored by the AE sensors. In this research, traditional AE analysis to compute AE parameters is applied to extract gear fault features.

7 AE parameters are computed as gear fault features: (1) ring-down count (2) duration (3) peak amplitude (4) rise time (5) rise time slope (6) RMS (7) Kurtosis. The ring-down count is defined as the number of threshold crossing made by an acoustic emission event. The duration is defined as the time between the initial rise of acoustic emission energy above the threshold and the time at which the acoustic emission energy decays below the threshold. The peak value is the absolute value of the highest voltage attained by a single acoustic emission event. The rise time is defined as the time between the initial crossing of the threshold and the time at which the peak amplitude occurs. The rise time slope is defined as the peak amplitude minus the threshold voltage divided by the rise time. RMS is defined by equation (3) and Kurtosis is defined by equation (4) as follows:

$$RMS = \sqrt{\frac{1}{n}\sum_{i=1}^{n}x_i^2} \qquad (3)$$

Where x_i is the signal.

$$Kurtosis = \frac{\frac{1}{n}\sum_{i=1}^{n}(x_i - \bar{x})^4}{(\frac{1}{n}\sum_{i=1}^{n}(x_i - \bar{x})^2)^2} \qquad (4)$$

where x_i is the signal and $\bar{x}$ is the mean value of the signal.

Totally 200 datasets were collected from the healthy gearbox and the value of the threshold is chosen to be 0.1 v based on the criteria that for acoustic emission signals of the healthy gearbox can seldom exceed this value. Waveforms of AE signals are selected based on the 7 AE parameters. There following criteria is used: the higher the rise time slope, ring-down count, duration, and peak amplitude, and the lower the rise time is, the more accurate the extracted waveform data is. To select the valid waveform, data point in the AE signal which finds relative maximum of the AE parameters is selected. The waveform corresponding to this point is selected as the valid waveform.

2.3 KNN based Fault Classification

KNN method is a simple passive machine learning algorithm. As shown in (He and Bechhoefer, 2008), KNN method was successfully applied to the bearing fault diagnostics and prognostics. KNN algorithm assumes all observations correspond to points in the p-dimensional space (He and Bechhoefer, 2008). The nearest neighbors of an observation are defined in terms of the standard Euclidean distance. Assume there are two vectors x_i, x_j, the Euclidean distance is defined in Eq. (5). An observation is classified by a majority vote of its neighbors.

$$E(x_i, x_j) = \sqrt{\sum_{k=1}^{p}(x_{ik} - x_{jk})^2} \qquad (5)$$

where x_{ik} and x_{jk} are elements that belong to the two vectors x_i, and x_j.

In this paper, the KNN method is used for STG fault classification based on gear fault features extracted by both HHT and AE analysis and the classification performance using both vibration based and AE based features are compared. The scheme of KNN algorithm based fault classifier is shown in Figure 5.
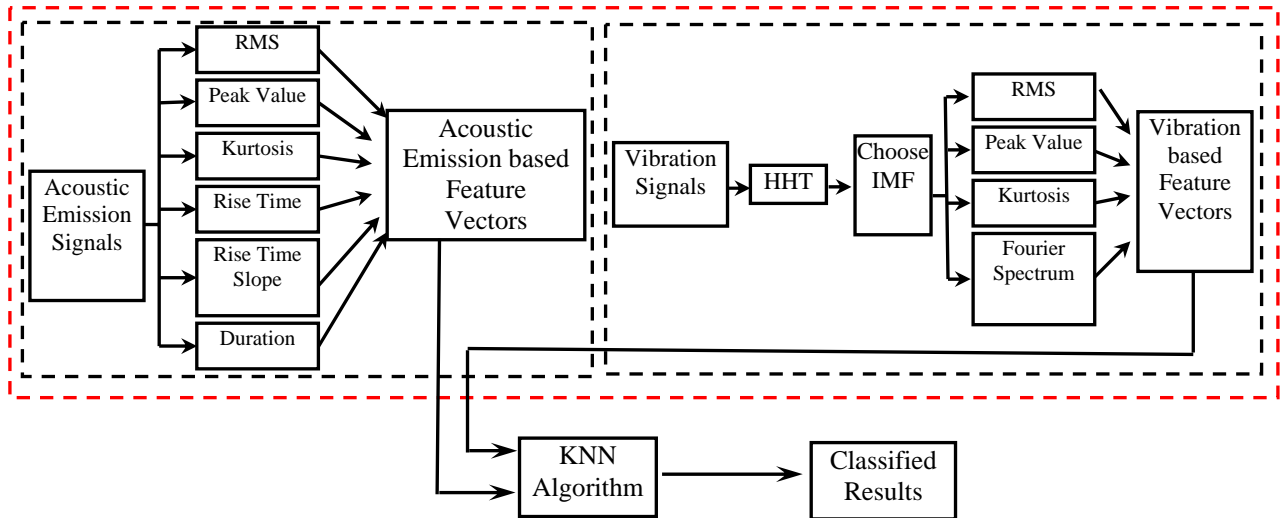

Figure 5: The scheme of the KNN method

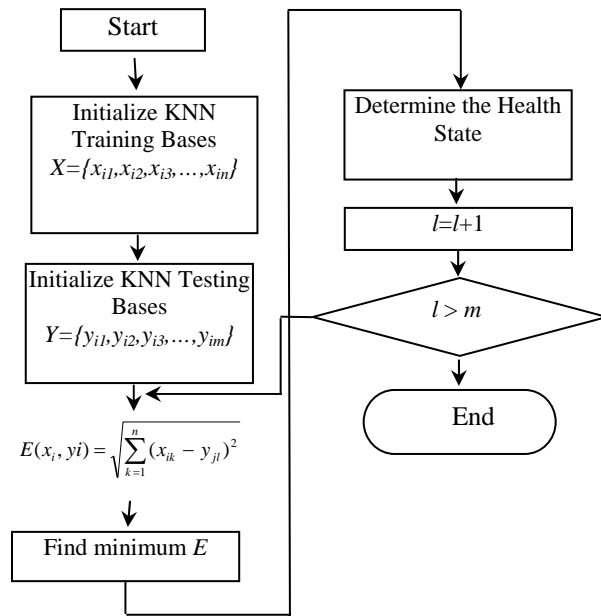The flowchart of KNN algorithm is shown in Figure 6.

Figure 6: The flowchart of the KNN algorithm

Figure 7: The split torque gearbox

(a)

(b)

Figure 8: (a) Input drive side and (b) output driven side of the STG

3   EXPERIMENTAL SETUP AND ANALYSIS RESULTS

In an effort to gain experience in performing HUMS types of analysis on STG, Goodrich working with the University of Illinois at Chicago (UIC) has built a test gearbox for the purpose of testing condition indicators (CI) used in HUMS and condition based maintenance practices. The primary design considerations were emulation of synchronous gear signals that would be found in a STG (see Figures 4 & 5). The STG type gearbox is driven by a 3-Hp AC motor and the maximum input rotational speed is 3600 rpm. A torque sensor is installed on the input shaft to measure the torque applied to the output shaft. On the input side of gearbox, the input driving gear is a 40-tooth gear, driving three driven spur gears of 72 teeth. On the output side, the output driving gears are three 48-tooth output spur gears which drive a single 64-tooth output driven gear. A magnetic loading system is connected to the output shaft of the output spur gear. The magnetic loading system is controlled by a power supply and the load can be adjusted by changing the output current of the amplifier.
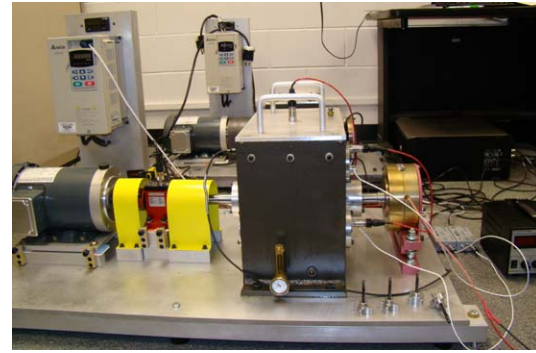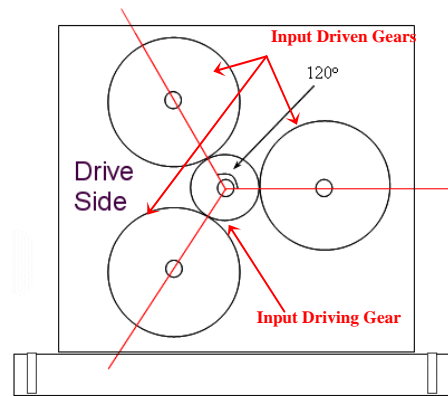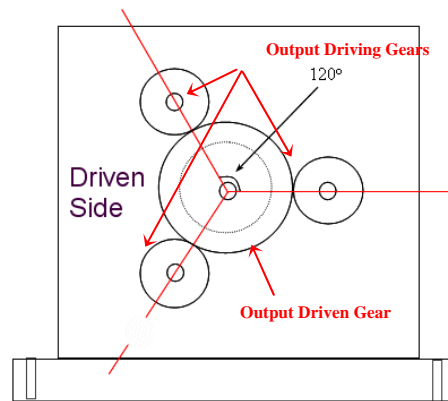
Three accelerometers were mounted on the input drive pinion and at the locations near the output driving gears and two acoustic emission sensors were mounted at the locations near the output driving gears. In the experiments, 20% of a tooth in one of the driving gears was chipped. The damaged gear is shown in Figure 9. The damaged gear is placed at location 2. The locations of the accelerometers and the acoustic emission sensors are shown in Figure 10. During the experiments, the input speed was kept at 3600 rpm.

The sampling rate for vibration signals was set to be 102.4 kHz. Vibration data for both the damaged gearbox and the healthy gearbox were collected. For each case, there were totally 200 datasets sampled. For AE signals, the sampling rate was set to be 5 MHz. AE data for both the damaged gearbox and the healthy gearbox were collected. For each case, there were totally 200 datasets sampled.
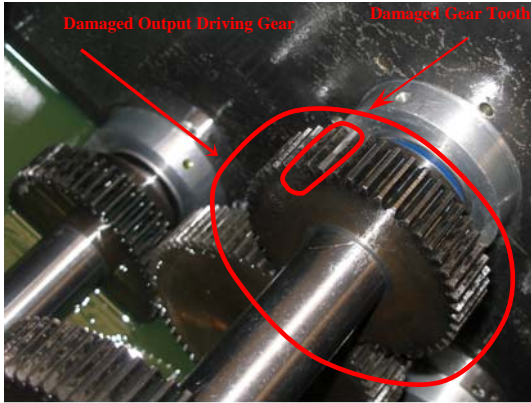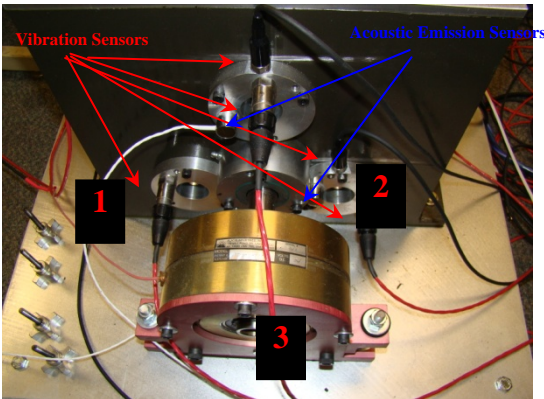

Figure 9: The Damaged Gear

Figure 10: The locations of vibration and acoustic emission sensors

3.1 Analysis Results of Vibration Signals

An example set of the healthy gearbox data is shown in Figure 11 (a). An example of the damaged gearbox data is shown in Figure 11 (b).
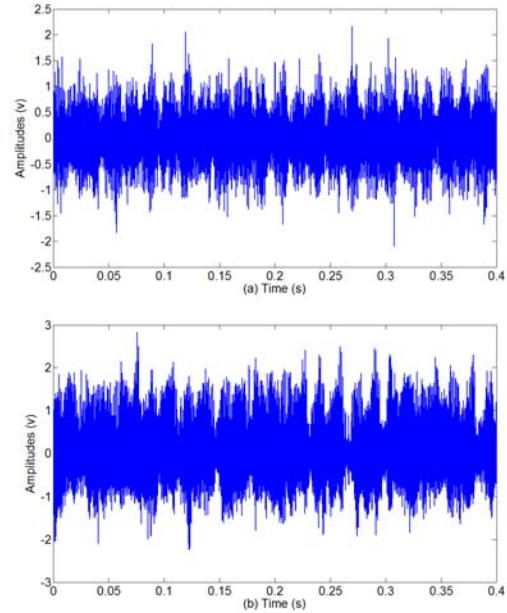

Figure 11: The vibration signals of the (a) healthy gearbox and (b) damaged gearbox

The HHT was applied to the vibration signals and the 3rd IMF component was chosen because of this IMF component was associated with the gear meshing frequency of 1600 Hz. The RMS, peak value, kurtosis, and the amplitude of the shaft frequency of the damaged gear in the Fourier spectrum of the 3rd IMF component were calculated as the features.

In our experiment, we first wanted to test whether the vibration can detect the fault in the gearbox. The features were extracted for every dataset for both the healthy gearbox and the damaged gearbox to generate 400 feature vectors. From the generated feature vectors, 150 of the healthy gearbox and 150 of the damaged gearbox were used as the training features to train the KNN classifier. Then the rest of the feature vectors were used for classification. The classification results are shown in Table 1. From Table 1, we can see that the classification accuracy is 95%.

Table 1: The confusion matrix for fault detection using vibration

	Predicted Classes	
Actual Classes	**Healthy Gearbox**	**Damaged Gearbox**
Healthy Gearbox	45	5
Damaged Gearbox	0	50

To see whether the vibration could locate the fault, the vibration signals collected at location 1 (healthy gear) and location 2 (damaged gear) were used.

Totally 200 data sets were sampled for both the sensor located at location 1 and location 2. The vibration signals were processed for both the healthy gear and the damaged gear to generate 400 feature vectors. From the generated feature vectors, 150 of the healthy gear and 150 of the damaged gear were used as the training features to train the KNN classifier. Then the rest of the feature vectors were used for classification. The classification results are shown in Table 2. From Table 2, we can see that the classification accuracy is 78%.

Table 2: The confusion matrix for fault location detection using vibration

	Predicted Classes	
Actual Classes	Location1	Location2
Location1	37	13
Location2	9	41

From Table 1 and Table 2, we can see that when using the vibration based fault features, the KNN algorithm can accurately classify the damaged gear state from the healthy gear state. However, for fault location detection, the vibration based fault features provide an accuracy of only 78%.

3.2 Analysis Results of the AE Waveforms

An example waveform of the healthy gearbox AE signal is shown in Figure 12 (a).
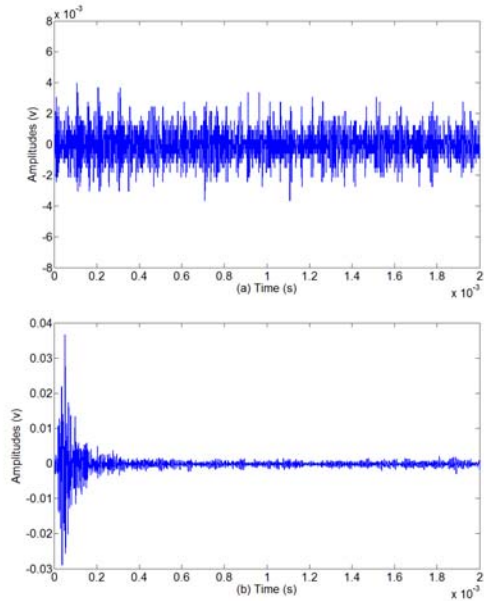
Figure 12: The acoustic emission signals of the (a) healthy gearbox and (b) damaged gearbox

Table 3 shows RMS, kurtosis, peak value, ring-down count, rise time, duration, and rise time slope of the AE signal in Figure 12.

Table 3: The features of the AE signals in Figure 11

	RMS (v)	Kurtosis (v)	Peak Value	Ring-down Count	Rising Time	Duration (ms)	Rise Time Slope
Healthy	0.004	4.550	0.015	——	——	——	——
Damaged	0.07	6.00	0.33	27	0.03	0.27	7667

The features shown in Table 3 were extracted for every dataset for both the healthy gearbox and the damaged gearbox to generate 400 feature vectors. From the generated feature vectors, 150 of the healthy gearbox and 150 of the damaged gearbox were used as the training features to train the KNN classifier. Then the rest of the feature vectors were used for classification. The classification results are shown in Table 4.

Table 4: The confusion matrix for fault detection using AE signals

	Predicted Classes	
Actual Classes	Healthy Gearbox	Damaged Gearbox
Healthy Gearbox	50	0
Damaged Gearbox	0	50

From Table 4, we can see that an accuracy of 100% to classify healthy or damaged state of the gearbox using AE signals was achieved. By comparing the results of AE and vibration, we can see that AE signals

are sensitive to the damage of the gear in the split torque gearbox. Moreover, the AE signals do not need sophisticated algorithm to generate the fault features.

To see whether the AE signals could locate the fault, the AE signals collected at location 1 (healthy gear) and location 2 (damaged gear) were used. Totally 200 datasets were sampled for both the AE sensors located at location 1 and location 2. Example waveforms of the AE signals are shown in Figure 12. From Figure 12 we can see the AE signals collected at the location 2 reflects more fault features than the signals collected at the location 1.

Table 5 shows RMS, kurtosis, peak value, ring-down count, rise time, duration, and rise time slope of the AE signal in Figure 12. The threshold was set to be 0.1 v.
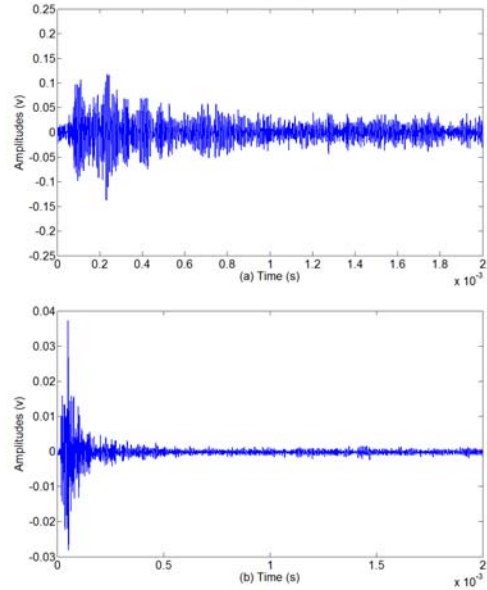

Figure 13: The acoustic emission signals (a) at location 1 and (b) at location 2

Table 5: The features of the acoustic emission signals of the damaged gearbox

	RMS (v)	Kurtosis (v)	Peak Value (v)	Ring-down Count	Rising Time (ms)	Duration (ms)	Rise Time Slope
Location 1	0.03	2.60	0.13	15	0.008	0.26	3750
Location 2	0.07	6.00	0.33	27	0.03	0.27	7667

To show the effectiveness of the damage source detection using AE signals, the AE parameters were extracted for both location 1 and location 2 AE signals to generate 400 feature vectors. From the generated feature vectors, 150 of location 1 and 150 of location 2 AE signals were used as the training features to train the KNN classifier. Then the rest of the feature vectors were used for classification. The classification results are shown in Table 6.

Table 6: The confusion matrix for fault location detection using AE signals

Actual Classes	Predicted Classes	
	Location1	Location2
Location1	49	1
Location2	2	48

The results in Table 6 show that 97% accuracy rate was achieved by using the AE signals to locate the fault source of the gearbox. In comparison with the 78% accuracy using vibration, AE approach performed significantly better in terms of identifying the source of the fault.

4   CONCLUSIONS

The benefits potentially offered by STG have driven the helicopter manufacturing community to develop products using the STG. However, this may pose a challenge for the current gear analysis methods used in HUMS. Gear analysis uses time synchronous averages to separates in frequency gears that are physically close to a sensor. The effect of a large number of synchronous components (gears or bearing) in close proximity may significantly reduce the fault signal (increase signal to noise) and therefore reduce the effectiveness of current gear analysis algorithms. Up to today, only a limited research on STG fault diagnosis has been conducted.

In this paper, we investigated fault diagnosis for STG using both vibration and acoustic emission (AE) signals. In particular, seeded fault tests on a STG type gearbox were conducted to collect both vibration and AE signals. Gear fault features were extracted from vibration signals using a Hilbert-Huang Transform (HHT) based algorithm and from AE signals using AE analysis, respectively. These fault features were used for fault detection using a K-nearest neighbor (KNN) algorithm. Our investigation has shown that the fault features extracted from both vibration and AE signals were capable of detecting the gear fault in a STG. However, in terms of locating the source of the fault, the fault features extracted from AE analysis outperformed those extracted from the vibration analysis.

REFERENCES

(Bechhoefer *et al.*, 2009) E. Bechhoefer, R. Li, and D. He. Quantification of Condition Indicator Performance on A Split Torque Gearbox, *American Helicopter Society 65th Annual Forum*, Grapevine, Texas, 2009.

(Eftekhamejad and Mba, 2009) B. Eftekharnejad and D. Mba. Seeded Fault Detection on Helical Gears with Acoustic Emission, *Applied Acoustics*, vol. 70, pp. 547 – 555., 2009.

(Gmirya, 2008) Y. Gmirya. Split Torque Gearbox for Rotor Wing Aircraft with Translational Thrust System, *USPTO*, 7,413,142, 2008.

(Hamzah and Mba, 2009) R.I.R. Hamzah and D. Mba. The Influence of Operating Condition on Acoustic Emission Generation during Meshing of Helical and Spur gear, *Tribology International*, vol. 42, pp. 3 – 14., 2009.

(He and Bechhoefer, 2008) D. He and E. Bechhoefer. Development and Validation of Bearing Diagnostic and Prognostic Tools Using HUMS Condition Indicators, *Proceedings 0f 2008 IEEE Aerospace Conference*, Big Sky, MT, 2008.

(Huang *et al.*, 1998) N. Huang, Z. Shen, S. Long, N. Wu, H. Shih, Q. Zheng, N. Yen, C. Tung, and H. Liu. The Empirical Mode Decomposition and the Hilbert Spectrum for Nonlinear and Non-stationary Time Series Analysis, *Proceedings of the Royal Society of London - A*, vol. 454, pp. 903 – 995., 1998.

(Krantz, 1995) T. Krantz. Vibration Analysis of A Split Path Gearbox. *NASA Technical Memorandum 106875*, AIAA-95-3048,1995.

(Krantz, 1996) T. Krantz. Code to Optimize Load Sharing of Split-Torque Transmissions Applied to the Comanche Helicopter,*grc.nasa.gov /WWW/RT /RT1995/2000/2730k.*, 1996

(Li and He, 2009) R. Li and D. He. Using Hilbert-Huang Transform for Gearbox Fault Detection under Light Loading Conditions, *Proceedings of the 2009 MFPT Conference*, Dayton, OH, 2009.

(Liu *et al.*, 2006) B. Liu, S. Riemenschneider, and Y. Xu. Gearbox Fault Diagnosis Using Empirical Mode Decomposition and Hilbert Spectrum, *Mechanical Systems and Signals Processing*, vol. 20, No. 3, pp. 718 - 734., 2006.

(Liu *et al.*, 2006) J. Liu, X. Wang, and S. Yuan, On Hilbert-Huang Transform Approach for Structural Health Monitoring, *Journal of Intelligent Material Systems and Structures*, vol. 17, No. 8-9, pp. 721 – 728., 2006.

(Tan *et al.*, 2007) C. Tan, P. Irving, and D. Mba. A Comparative Experimental Study on the Diagnostic and Prognostic Capabilities of Acoustics Emission, Vibration and Spectrometric Oil Analysis, *Mechanical Systems and Signal Processing*, vol. 21,pp. 208 – 233.

(Tang *et al.*, 2007) J. Tang, Q. Zou, Y. Tang, B. Liu, and X. Zhang. Hilbert-Huang Transform for ECG De-noising, *2007 1st International Conference on Bioinformatics and Biomedical Engineering*, Wuhan, Hubei, China., 2007.

(Toutountzakis *et al.*, 2005) T. Toutountzakis, C. Tan, and D. Mba. Application of Acoustic Emission to Seeded Gear fault Detection, *NDT&E International*, vol. 38, pp. 27 -36., 2005.

(Wang *et al.*, 2001) W. Wang, F. Ismail, and F. M. Golnaraghi. Assessment of Gear Damage Monitoring Techniques Using Vibration Measurements, *Mechanical Systems and Signal Processing*, vol. 15, No. 5, pp. 905 – 922. , 2001.

(White[1], 1982) G. White. Design Study of Split-torque Helicopter Transmissions, *NASA Technical Report*, NAS3-22528., 1982.

(White[2], 1982) G. White. Split Torque Transmission. *USPTO*, 4,489,625, 1982.

(Yan and Gao, 2006) R. Yan and R. Gao. Hilbert-Huang Transform-based Vibration Signals Analysis for Machine Healthy Monitoring, *IEEE Transactions on Instrumentation and Measurement*, vol. 55, No. 6, pp. 2320 – 2329., 2006.

Ruoyu Li was born in Jan. 28th, 1980 in Leshan, Sichuan Province, China. He received his B.S. and M.S. degrees in automatic control and control theory and control engineering from The Guilin University of Electronic Technology, Guilin,

Guangxi, China in 1998 and 2002, respectively. He is a Research Assistant in the Intelligent Systems Modeling and Development Laboratory and working toward his Ph.D. degree in the Department of Mechanical & Industrial Engineering at The University of Illinois-Chicago. His research interests include machine condition monitoring and fault diagnosis and sensors networks, advanced digital signal processing, and mechatronics systems design.

Dr. David He is an Associate Professor and the Director of The Intelligent Systems Modeling & Development Laboratory in the Department of Mechanical & Industrial Engineering at The University of Illinois-Chicago. His research interests include: equipment health diagnostics and prognostics, wireless sensor network modeling and analysis, systems reliability modeling and analysis, statistical quality control, manufacturing scheduling.

Dr. Eric Bechhoefer is a Fellow at Goodrich SIS and retired Naval aviator with a M.S. in Operation Research and a Ph.D. in General Engineering, with a focus on Statistics and Optimization. Dr. Bechhoefer has worked at Goodrich Aerospace since 2000 as a Diagnostics Technical Lead. He has previously worked at The MITRE Corporation in the Signal Processing Center.